UCRL-CONF-230182

LAWRENCE
LIVERMORE
NATIONAL
LABORATORY

In situ Investigation of the Silver-CTAB system

J. J. Gray, C. A. Orme, D. Du, D. Srolovitz

April 23, 2007

Disclaimer

In situ Investigation of the Silver-CTAB system

Jeremy Gray[1], Christine Orme[2], Danxu Du[3], and David Srolovitz[4]

[1]CMLS, Lawrence Livermore National Laboratory, 7000 East Ave, Livermore, CA, 95550
[2]LLNL, Livermore, CA, 94550
[3]Princeton, Princeton, NJ, 08540
[4]Yeshiva University, New York, NY, 10033

ABSTRACT

Recent research has shown that biologically inspired approaches to materials synthesis and self-assembly, hold promise of unprecedented atomic level control of structure and interfaces. In particular, the use of organic molecules to control the production of inorganic technological materials has the potential for controlling grain structure to enhance material strength; controlling facet expression for enhanced catalytic activity; and controlling the shape of nanostructured materials to optimize optical, electrical and magnetic properties. In this work, we use organic molecules to modify silver crystal shapes towards understanding the metal-organic interactions that lead to nanoparticle shape control.

Using in situ electrochemical AFM (EC-AFM) as an in situ probe, we study the influence of a cationic surfactant cetyltrimethylamminobromide (CTAB) on Ag growth during electrochemical deposition on Ag(100). The results show that the organic surfactant promotes the growth of steps on the (100) surface and changes the surface evolution from island nucleation to step flow growth. Overall, this leads to a smoother, faster growing (100) surface, which may promote plate-formation.

INTRODUCTION

Recently, the metal-organic modulation of nanocrystals composed of metals and metal-oxides have garnered much interest. Because of their size, surface area, and unique properties, there is great interest in the use of metal and metal-oxide nanoparticles for a wide range of technological applications. Tight control of shape and size are very important for these applications. For example, the optical properties of gold and silver depend sensitively on their shape and size. The plasmon resonance can be tuned from red to blue by adjusting size, and the aspect ratio of the nanoparticles determines the coupling with longitudinal and transverse light waves. In a similar manner the magnetic properties of nickel and iron particles can be tailored by changing the shape from a sphere to a rod. Nanocrystals are also being utilized in catalysis and remediation due to their high surface area. In these applications, the facet expression and the step structure determines the overall chemical activity and, therefore, shape is crucial to function.

Several studies have shown that CTAB can be used to create silver nanorods and nanoplates[1-3]. These include several studies at room temperature where the mechanisms for shape change appear to depend upon CTAB concentration. At high concentrations of CTAB (~0.1M) it is suggested that shape control is due to the structure of the surfactant gel and promotes nanorod formation. At lower concentrations of CTAB (.006M) growth lead to {111} dominated plates with a truncated triangular morphology. By contrast in the absence of growth modifiers silver nanoparticles have a morphology dominated by {111} and {100} facets as dictated by their surface energy. Chen & Carroll suggest that shape control at the lower CTAB

concentration is due to the preferential adsorption of CTAB on the {111} facet of Ag and the formation of AgBr. To create a shape dominated by {111} facets, either the {111} facet growth rate is reduced or the other facet directions speed up.

In the experiments described in this proceedings we use in situ AFM to monitor the effect of CTAB on the (100) face of Ag, to help develop a mechanistic understanding of one piece of this process. In this study we use low concentrations of CTAB (0.0005M) closer to studies forming plates rather than rods.

EXPERIMENT

Single crystal Ag(100) samples with a purity of 99.999% (Matech, Julich, Germany) were mechanically polished with pastes of progressively smaller alumina particle sizes down to 50nm. Following mechanical polishing, the samples were chemically etched in a solution containing 4.8% CrO_3, 4% HCl and 20% $HClO_4$, followed by a 20s immersion in concentrated H_2SO_4 and then 300s in a solution containing 25% NH_3. Following the chemical etch, the sample was rinsed thoroughly in ultrapure water (Millipore-Q).

Electrochemical deposition experiments were performed using a solution of 0.1M HNO_3 + 0.002M $AgNO_3$. Ultra-high purity HNO_3 (99.9999%) and $AgNO_3$ (99.99995%) were purchased from Alfa Aesar. CTAB (99.9%) was added to the growth solutions in situ to concentrations of 0.5mM.

AFM measurements were performed using a multi-mode (Digital Instruments, Santa Barbara, CA) operating in contact mode. The in situ cell was equipped with three ports to allow for electrochemical deposition. A high purity (99.999%) silver wire was used as the reference electrode and a platinum wire served as the counter electrode. A potentiostat (Gamry Instruments, Warminster, PA) was used to control the deposition potential and record the resultant current.

DISCUSSION
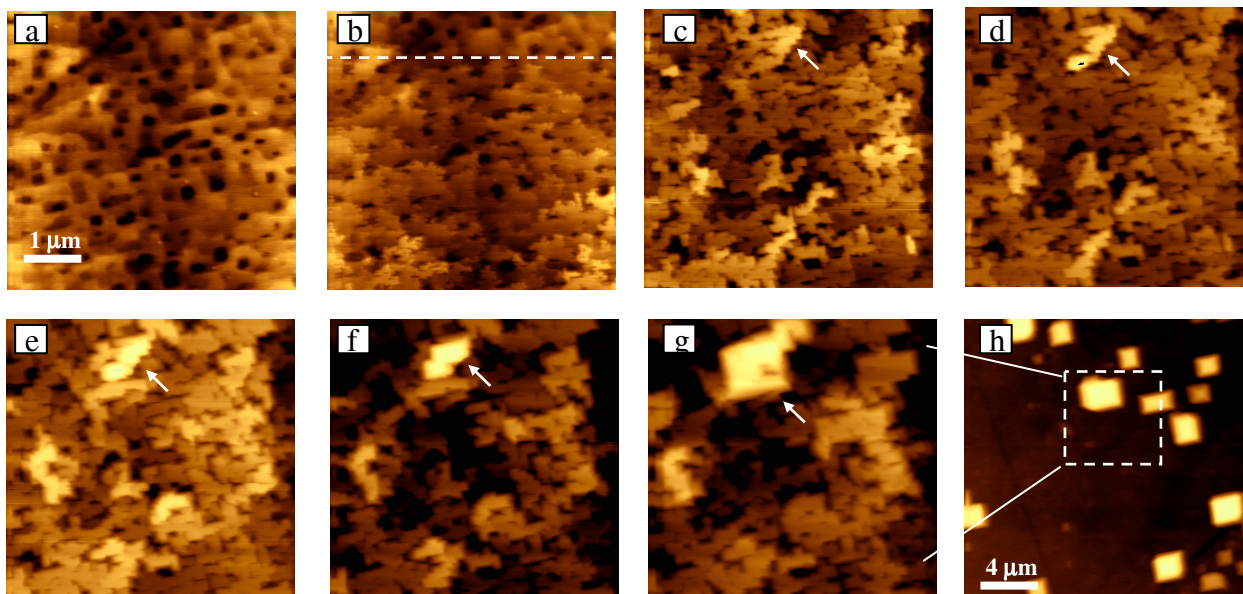
Ag electrodeposition on Ag(100)

Fig. 1. AFM topographs of the time evolution of silver growth by electrodeposition on Ag(100) in a solution containing 0.1M HNO$_3$ + 2mM AgNO$_3$ (no organic modifier). (a) The resultant surface morphology following the chemical polishing procedure. (b) The dashed line indicates the time when a potential of 10mV vs. the silver wire reference electrode, was applied resulting in a deposition current of ~ 10μA/cm^2. (c) through (g) show the time evolution (1min per scan) of silver growth, where the arrows indicate the location of an island. (h) Shows the resultant surface morphology on a larger (20 micron) scale.

Fig. 1 shows AFM topographs of the time evolution of silver growth by electrodeposition on Ag(100) in 0.1M HNO$_3$ + 2mM AgNO$_3$. Fig. 1(a) shows the Ag(100) surface after the polishing procedure detailed above. The in-plane [100]-orientations can clearly be seen from the square etch-pits that result from the chemical polish and the resultant morphology consists of many large terraces (> 100nm). Figs. 1(b) through 1(g) show the time evolution of silver electrodeposition. The dashed line indicates the time when a potential of 10mV vs. the silver wire reference electrode, was applied resulting in a deposition current of ~ 10μA/cm^2. Each image is taken in sequence and the image acquisition time is 45 seconds. From the time sequence, the growth immediately following deposition is appears dendritic due to the short step segments but eventually follows a preferred growth along the [100] directions. The arrows in Figs. (c) through (g) indicate the location of nucleation and growth of an Ag island. As can be seen in the figure, the growth eventually evolves into an epitaxial 100-faceted crystal. Following the time sequence acquisition, a larger area scan was acquired. The resultant surface morphology is shown in Fig. 1(h). The image shows that the Ag(100) surface is sparsely covered with Ag islands that are each aligned along the in-plane [100] directions.

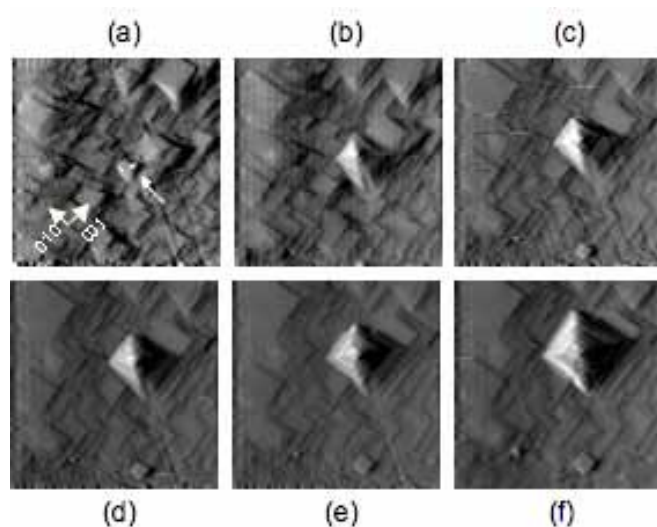**Ag electrodeposition on Ag(100) in the presence of the organic surfactant CTAB**

Fig. 2. AFM deflection (a-f) and three-dimensional topographic (a'-f') images of the time evolution of silver growth by electrodeposition on Ag(100) in a solution containing 0.1M HNO$_3$

+ 2mM AgNO$_3$ + 0.5mM CTAB. (a) The resultant surface morphology following the chemical polishing procedure where the arrow indicates the location of hillock formation. (b) Image acquired after two minutes of deposition at a potential of 10mV vs. the silver wire reference electrode, which resulted in a deposition current of ~ 7μA/cm^2. (c) through (f) show the time evolution (1min per scan) of silver growth.

Fig. 2 shows AFM deflection (a-f) images of the time evolution of silver growth by electrodeposition on Ag(100) in a solution containing 0.1M HNO$_3$ + 2mM AgNO$_3$ + 0.5mM CTAB. From the figure, it can be seen that Ag growth is significantly altered in the presence of CTAB. In contrast to the growth in the absence of CTAB, the Ag surface does not grow dendritically. Rather, the in-plane orientations of the growing steps are aligned with the 010 and 001 directions of the substrate (as indicated in Fig. 2a). Instead of forming faceted islands the surface forms shallow pyramidal hillocks, where the base of the pyramid is aligned with the underlying substrate. The arrow in Fig. 2a and b indicate the location of a nucleation site for Ag hillock growth.

In situ addition of CTAB into Ag growth solution

Fig. 3 shows the influence of CTAB on islands nucleated in the pure growth solution. Fig. 3a shows a three-dimensional view of the surface of Ag(100) during electrodeposition in 0.1M HNO3 + 2mM AgNO3 leading to faceted Ag island nucleation and growth. Also shown in the figure (Fig. 3f) is a plane view of the surface showing that the resultant growth in the absence of CTAB leads to island growth which display primarily {100} and {111} facets. Following nucleation of the faceted islands, 0.5mM CTAB was added to the growth solution in situ. The subsequent surface morphology during growth is shown in 3(b) through (e). As can be seen from the image sequence, the addition of CTAB leads to an increase in the substrate growth rate along the surface normal direction ((100)). As a result, the initially nucleated (faceted) islands slowly transition to shallow pyramidal hillocks with steps along the in-plane {100} directions, as shown by the black arrows in the plane-view of the surface (Fig. 3(g)).

The lengthening and smoothing of the steps within the (100) surface is consistent with an increase in the diffusion rate of Ag+ ions on the surface. In this case, one would expect Ag adatoms to find more global minima at step edges rather than nucleating new islands leading to a transition from island nucleation to step flow growth. In addition, increased diffusion along step-edges would tend to straighten steps, reducing the kink density.
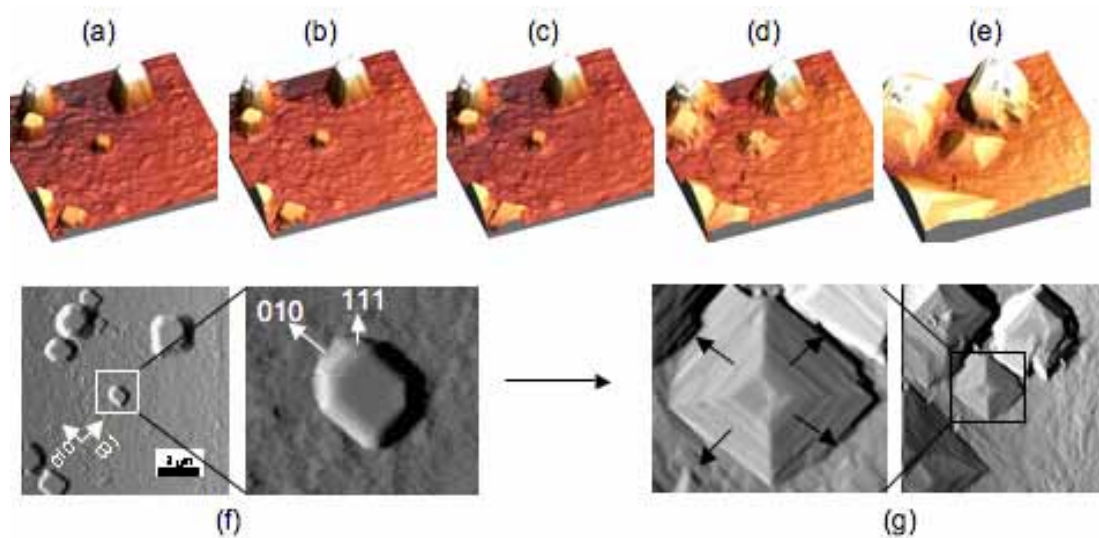
Fig. 3. (a-c) show the time evolution of the growth of Ag islands without the organic modifier CTAB. (d-l) show the resultant temporal evolution of the Ag islands following the addition of 0.5mM CTAB. Each scan was completed in approximately 1 minute and the time between the acquired images was 1 minute as well.

CONCLUSIONS

The effect of CTAB on the (100) facet is to transition the growth from island nucleation to step flow growth and to smoothen and lengthen the steps. Both effects are consistent with a higher mobility of Ag adatoms on the surface. As a result, the entire substrate begins to grow and the surface becomes dominated by [100] steps that eventually merge leading to an overall smother surface. In addition, the growth rate of the {100} facet increases in the presence of the CTAB. As the shape of crystals is due to the relative growth rates of the different crystallographic planes, an increase in growth rate of the {100} face relative to the {111} face may contribute to the formation of plate-like structures as observed in Ag/CTAB nanoparticle synthesis.

ACKNOWLEDGMENTS

REFERENCES

1. Chen, S. & Carroll, D. *J. Phys.Chem. B*, 108, 5500, (2004).
2. Lee, G., Shin, S., Kim, Y.C., Oh, S.-G., Mater Chem Physics, 84, 197, (2004).
3. Nikoobakaht, B., El-Sayed, M., Langmuir, 17, 6368, (2001).